Journal of Alloys and Compounds 471 (2009) 60–63

Contents lists available at ScienceDirect

Journal of Alloys and Compounds

journal homepage: www.elsevier.com/locate/jallcom

The isothermal section of the Ce–Co–Sb ternary system at 400 °C

R.M. Luo, F.S. Liu, J.Q. Li*, X.W. Feng

College of Materials Science and Engineering, Shenzhen University and Shenzhen Key Laboratory of Special Functional Materials, Shenzhen 518060, PR China

ARTICLE INFO

Article history:
Received 7 December 2007
Received in revised form 12 March 2008
Accepted 12 March 2008
Available online 9 May 2008

Keywords:
Rare earth alloys and compounds
Phase diagram
X-ray powder diffraction

ABSTRACT

Phase equilibria were established in the Ce–Co–Sb ternary system at 400 °C based on X-ray powder diffraction (XRD), scanning electron microscopy (SEM) and energy dispersion spectroscopy (EDS) techniques. Fourteen binary compounds $Ce_{24}Co_{11}$, $CeCo_2$, $CeCo_3$, Ce_2Co_7, Ce_5Co_{19}, Ce_2Co_{17}, CoSb, $CoSb_2$, $CoSb_3$, Ce_2Sb, Ce_5Sb_3, Ce_4Sb_3, CeSb and $CeSb_2$ have been confirmed, and three ternary compounds $CeCoSb_3$, $CeCo_{1-x}Sb_2$ and $CeCo_{1.33}Sb_2$ are found in this system at 400 °C. The isothermal section of this system at 400 °C consists of 20 single-phase regions, 40 two-phase regions and 21 three-phase regions. The compound $CeCo_{1-x}Sb_2$ has $ZrCuSi_2$-type structure with space group *P4/nmm*, $a = 0.3878$ nm and $c = 0.9849$ nm. The crystal structure for the compound $CeCoSb_3$ is determined to be $CeNiSb_3$-type (*Pbcm*) with $a = 1.27697$ nm, $b = 0.60601$ nm and $c = 1.8435$ nm. The compound $CeCo_{1.33}Sb_2$ is of orthorhombic system with $a = 0.6083$ nm, $b = 0.60118$ nm and $c = 1.04596$ nm. The homogeneity range of CoSb phase is about 2 at.%. The solubilities for the other single-phase regions were not observed.

1. Introduction

The Co–Sb system is drawing more and more attention due to its special feature found in recent years. The compound $CoSb_3$ in this system has the typical skutterudite structure exhibiting excellent transport properties, such as extremely high carrier mobility, that are desirable for good thermoelectric performance [1,2]. Rare earth-filled skutterudites have been identified as potential thermoelectric materials due to their reduced thermal conductivity [3,4]. Understanding the phase relationships of Re–Co–Sb system is helpful for the development of relative materials. The investigations of phase diagrams of the Eu–Co–Sb [5], Gd–Co–Sb [6], Nd–Co–Sb [7] and Pr–Co–Sb [8] have been reported, while no reports have been found on the interaction in the Ce–Co–Sb ternary systems. In this work, we investigated the phase equilibria in the Ce–Co–Sb ternary system at 400 °C.

2. Experimental detail

Cerium (purity of 99.99%), antimony (purity of 99.95%) and cobalt (purity of 99.99%) were used as raw materials. The alloys with 40 at.% Sb or more were prepared by high frequency melting under a high purity argon in quartz tube which was first evacuated to high vacuum to avoid the weight lost of the samples owing to the high volatility of antimony. The alloys with the Sb content less than 40 at.% were prepared in an electric arc furnace using a non-consumable tungsten electrode and a water-cooled copper tray under the protection of a pure argon atmosphere. The alloys were re-melted two or three times in order to achieve complete fusion and homogeneous composition. All samples were subjected to annealing for homogenization in evacuated quartz ampoules in a resistance furnace. The homogenization temperatures of the alloys were chosen on the basis of the binary phase diagrams of the Ce–Sb, Ce–Co and Sb–Co systems. The homogenization was performed at 600 °C for 20 days for the samples containing equal to or more than 40 at.% Sb, while at 900 °C for 15 days for the samples containing less than 40 at.% Sb. They are all then cooled to 400 °C at the rate of 10 °C/min, kept at 400 °C for 3 days and subsequently quenched into liquid nitrogen. 118 alloy samples in total were prepared for this investigation.

The treated alloys were powdered for X-ray powder diffraction (XRD) analysis. The phases in each alloy were identified by XRD with Cu Kα radiation (Bruker, D8 Advance SS 18 kW) and JADE 5.0 software. The software Topas 3.0 was used for Rietveld refinement [9]. The morphology and composition of the phase were investigated using a cold field emission scanning electron microscope (SEM) with energy dispersive analysis (EDS) (HITACHI S-4700).

3. Results and discussion

3.1. Phase analysis

We have studied the binary systems Co–Sb, Ce–Co and Ce–Sb at 400 °C to identify the binary compounds. The X-ray diffraction analysis confirmed the existence of the 14 binary compounds in the Ce–Co–Sb ternary system at 400 °C: $Ce_{24}Co_{11}$, $CeCo_2$, $CeCo_3$, Ce_2Co_7, Ce_5Co_{19} and Ce_2Co_{17} in the Ce–Co system; CoSb, $CoSb_2$ and $CoSb_3$ in the Co–Sb system; Ce_2Sb, Ce_5Sb_3, Ce_4Sb_3, CeSb and $CeSb_2$ in the Ce–Sb system. The binary compounds found in this work are in well agreement with those compounds reported in the literatures for Ce–Co [10], Co–Sb [11] and Ce–Sb [12] binary systems. The structure types and lattice parameters of these com-

* Corresponding author. Tel.: +86 755 26538528; fax: +86 755 26536239.
E-mail address: junqinli@szu.edu.cn (J.Q. Li).

0925-8388/$ – see front matter © 2008 Elsevier B.V. All rights reserved.
doi:10.1016/j.jallcom.2008.03.061

Table 1
Structure data and temperature of the phase transition of compounds in the Ce–Co–Sb ternary system

Compounds	Space group	Structure type	Lattice parameters (nm)			T^a (°C)	Reference
			a	b	c		
$Ce_{24}Co_{11}$	$P6_3mc$	$Ce_{24}Co_{11}$	0.9587	–	2.1825	**446**	[19]
$CeCo_2$	$FD\bar{3}m$	Cu_2Mg	0.7160			1036	[19]
Ce_2Co_7	$P6_3/mmc$	Ce_2Ni_7	0.4949	–	2.449	1130	[19]
$CeCo_3$	$R\bar{3}m$	Be_3Nb	0.4952	–	2.473	1103	[19]
Ce_5Co_{19}	$R\bar{3}m$	Ce_5Co_{19}	0.49475	–	4.87434	1134	[19]
Ce_2Co_{17}	$P6_3/mmc$	Th_2Ni_{17}	0.83779	–	0.81373	1204	[19]
CoSb	$P6_3/mmc$	NiAs	0.3890		0.5187	**1220**	[19]
$CoSb_2$	$Pnnm$	$CoSb_2$	0.65051	0.63833	0.65410	936	[19]
$CoSb_3$	$Im3$	$CoAs_3$	0.90385			874	[19]
Ce_2Sb	$I4/mmm$	La_2Sb	0.4552		1.784	1240	[19]
Ce_5Sb_3	Mn_5Si_3	P62/mcm	0.931		0.652	1440	[19]
Ce_4Sb_3	P_4Th_3	$I\bar{4}3d$	0.9511			1600	[19]
CeSb	$P4/mmm$	HgMn	0.3975	–	0.3244	1800	[19]
$CeSb_2$	$Cmca$	Sb_2Sm	0.628	0.613	1.824	1500	[19]
$CeCoSb_3$	$Pbcm$	$CeNiSb_3$	1.2769	0.6060	1.8435	–	This work
$CeCo_{1-x}Sb_2$	$P4/nmm$	$ZrCuSi_2$	0.3878		0.9849	–	[14]
$CeCo_{1.33}Sb_2$	$C222_1$	-	0.6083	0.6011	1.0459	–	This work

[a] Temperatures listed refer to phase transition or to the melting temperature (bold).

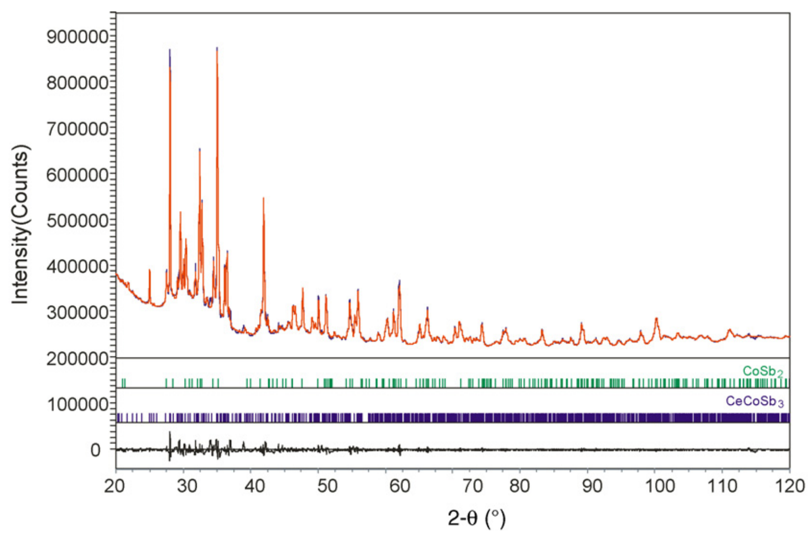

Fig. 1. Rietveld refinement result of the XRD pattern of the sample consisted of the compound $CeCoSb_3$ with small amount of $CoSb_2$ impurity.

pounds are listed in Table 1. Buschow [13] and Wu et al. [10] reported that the compound $CeCo_5$ decomposes into Ce_5Co_{19} and Ce_2Co_{17} by eutectoid reaction at a lower temperature (750 °C). Although the compound $CeCo_5$, as well as the compounds Ce_2Co_{17} and Ce_5Co_{19}, were found from XRD in the sample with composition of Ce–16.7Co–83.3($CeCo_5$) at 400 °C, the compound $CeCo_5$ is believed to be metastable at 400 °C and should not be presented in this isothermal section.

Three ternary compounds, $CeCoSb_3$, $CeCo_{1-x}Sb_2$ and $CeCo_{1.33}Sb_2$, were found in this Ce–Co–Sb ternary system at 400 °C. The compound $CeCo_{1-x}Sb_2$ has $ZrCuSi_2$-type structure [14] with space group $P4/nmm$, a = 0.3878 nm and c = 0.9849 nm. The Rietveld refinement performed using the Topas program for the XRD patterns of the sample, consisted of the new ternary compound $CeCoSb_3$ mainly, together with a small amount of CoSb, shows that the compound $CeCoSb_3$ is of $CeNiSb_3$-type [15] structure with the space group $Pbcm$, a = 1.27697 nm, b = 0.60601 nm and c = 1.8435 nm. The calculated data and differences of the powder diffraction patterns of $CeCoSb_3$ are shown in Fig. 1. For another new ternary compound with the possible chemical formula as $CeCo_{1+x}Sb_2$, we could not obtain its pure phase pattern. Fig. 2 shows the XRD patterns of the sample with composition of Ce–10Co–42Sb-48 consisted of the patterns of this new phase and the compound CoSb. The structure of this new phase is still unknown, but its XRD pattern has been successfully indexed by Topas 3.0 software [16] with a possible space group $Ccc2$,

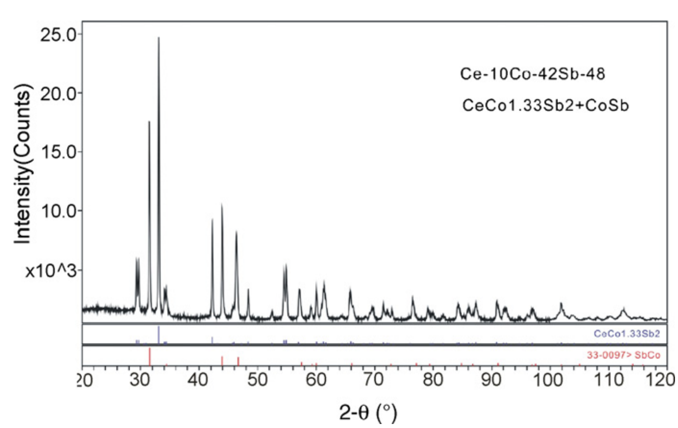

Fig. 2. XRD patterns of the samples with composition of Ce–10Co–42Sb-48 consisted of the compound $CeCo_{1.33}Sb_2$ and the CoSb phase.

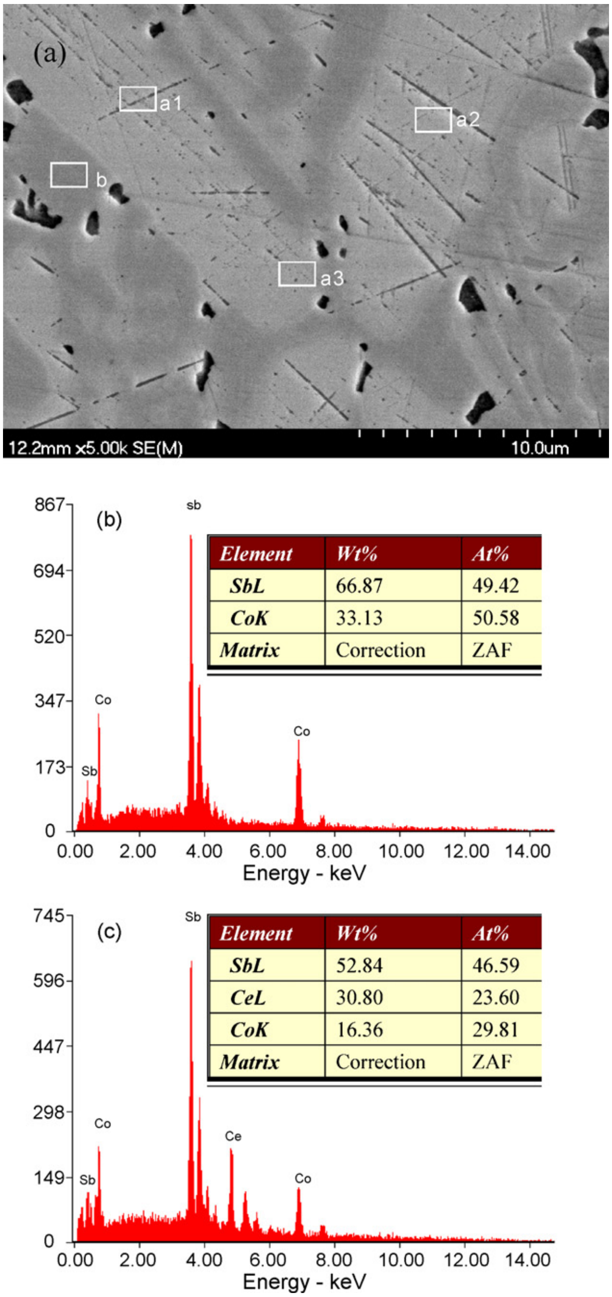

Fig. 3. SEM micrographs of the sample with composition of Ce–10Co–42Sb-48 (a) and EDS patterns for the dots labeled with b (b) and a1 (c) in (a).

$a = 0.60830$ (3) nm, $b = 0.60118$ (3) nm and $c = 1.04596$ (5) nm, the figure of merit M(19) of this indexing is equal to 16.9. In order to determine the exact chemical composition of this compound, a SEM and EDS analysis are performed for the sample with composition of Ce–10Co–42Sb-48, shown in Fig. 3. The SEM image shows that the alloy consists of two-phase regions, the darker grey region and bright grey region, representing two phases existed in this alloy. The EDS results show that the chemical composition of the darker grey region is 50.58 at.% Co and 49.42 at.% Sb, without any Ce detected (Fig. 3(b)), corresponding to CoSb phase. It also reveals that the solid solubility of Ce in the CoSb phase could not be detected. The chemical composition values, listed in Table 2, from EDS analysis at a1 (Fig. 3(c)) to a3 three dots for brighter grey region labeled in Fig. 3(a), are very close to each other with

Table 2
Chemical composition of the sample Ce–10Co–42Sb-48 obtained by EDS

No.	Ce (at.%)	Co (at.%)	Sb (at.%)
a_1	23.60	29.81	46.59
a_2	22.09	31.10	46.81
a_3	22.83	30.67	46.50
Average (a_1, a_2, a_3)	22.84	30.53	46.63
b	0	50.58	49.42

an average value of 22.84 at.% Ce, 30.53 at.% Co and 46.63 at.% Sb, which reveals that the chemical formula of the new compound is $CeCo_{1.33}Sb_2$. This phase is also found in the samples located in the other three-phase regions, such as the sample Ce–15Co–35Sb-50 located in the $CoSb + CeCo_{1-x}Sb_2 + CeCo_{1.33}Sb_2$ three-phase region (Fig. 4). No movement of XRD pattern of this phase was found in the samples with varying compositions, which indicated that there is no solubility range for this compound. The structure types and lattice parameters of the ternary compounds are also listed in Table 1.

3.2. Isothermal section at 400 °C of the Ce–Co–Sb ternary system

By comparing and analyzing the X-ray diffraction patterns of all samples, and identifying the phases present in each sample, we determined the phase equilibria in the Ce–Co–Sb ternary system and constructed its isothermal section at 400 °C, as shown in Fig. 5. It is consisted of 20 single-phase regions, 40 two-phase regions and 21 three-phase regions. The twenty single-phase regions are: Ce, Co, Sb, $Ce_{24}Co_{11}$, $CeCo_2$, $CeCo_3$, Ce_2Co_7, Ce_5Co_{19}, Ce_2Co_{17}, CoSb, $CoSb_2$, $CoSb_3$, Ce_2Sb, Ce_5Sb_3, Ce_4Sb_3, CeSb, $CeSb_2$, $CeCoSb_3$, $CeCo_{1-x}Sb_2$ and $CeCo_{1.33}Sb_2$.

The compound CoSb forms solid solutions by the way of substitution of Co atoms for Sb atoms at high temperature, but the homogeneity range decreases with temperature decrease. The homogeneity range of CoSb is about 2.0 at.% Sb at 400 °C [17]. The maximum solid solubility of Ce in CoSb could not be detected (see Fig. 3(b)). The maximum solid solubility of Ce in $CoSb_3$ at 400 °C is very small. The XRD pattern for the sample with composition of $Ce_{1.2}Co_{24.7}Sb_{74.1}$, shown in Fig. 6, consists of the patterns of a small amount of $CeSb_2$ and $CoSb_2$ phases as well as $CoSb_3$ main phase, indicating the maximum solid solubility of Ce in $CoSb_3$ at 400 °C is

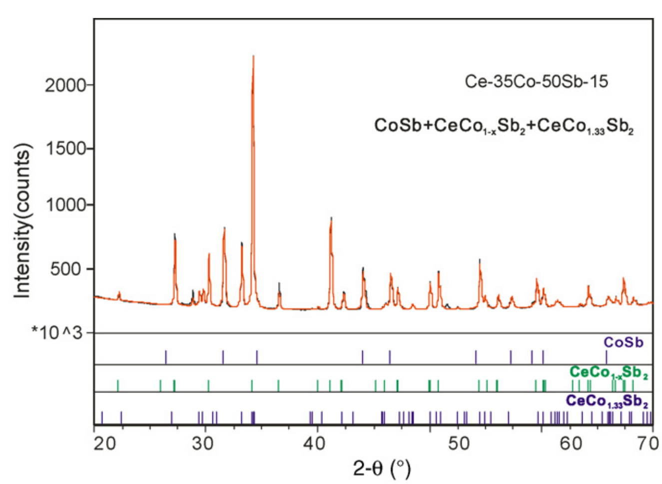

Fig. 4. XRD pattern of the sample with composition of Ce–15Co–35Sb-50 located in the $CoSb + CeCo_{1-x}Sb_2 + CeCo_{1.33}Sb_2$ three-phase regions showing the XRD pattern of the compound $CeCo_{1.33}Sb_2$.

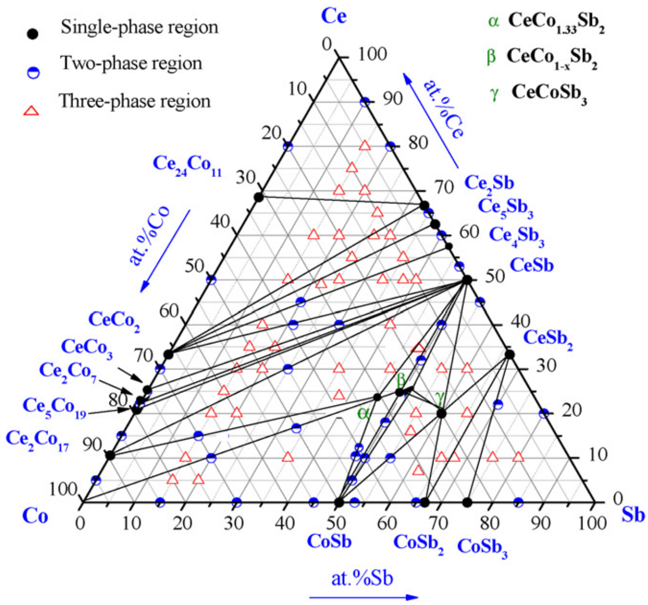

Fig. 5. Isothermal section of the phase diagram of the Ce–Co–Sb ternary system at 400 °C.

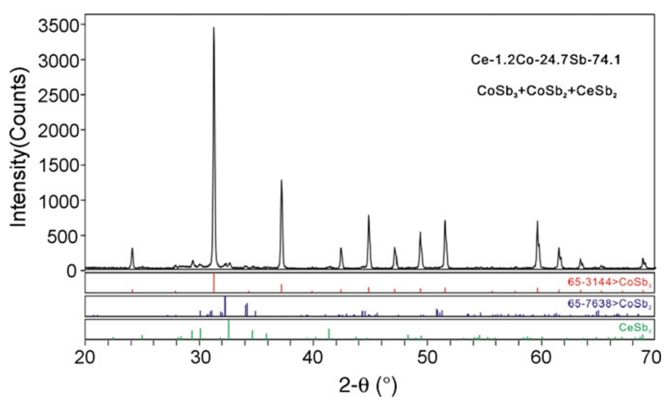

Fig. 6. XRD pattern for the sample with composition of Ce–1.2Co–24.7Sb-74.1, showing small amount of $CoSb_2$ and $CeSb_2$ appearing in the alloy.

less than 1.0 at.%. Mei et al. [18] reported that the filling limit of Ce in Co_4Sb_{12} by ab initio approach was 0.1 (about 0.7 at.% Ce). Such small solid solubility cannot be detected by XRD. The homogeneity ranges of the other single-phase regions are non-observable.

4. Conclusion

We have investigated and constructed the isothermal section of the Ce–Co–Sb ternary system at 400 °C. It is consisted of 20 single-phase regions, 40 two-phase regions and 21 three-phase regions. 14 binary compounds are: $Ce_{24}Co_{11}$, $CeCo_2$, $CeCo_3$, Ce_2Co_7, Ce_5Co_{19}, Ce_2Co_{17}, CoSb, $CoSb_2$, $CoSb_3$, Ce_2Sb, Ce_5Sb_3, Ce_4Sb_3, CeSb and $CeSb_2$. Three ternary compounds were found, they are $CeCoSb_3$ (*Pbcm*, $a = 1.27697$ nm, $b = 0.60601$ nm and $c = 1.8435$ nm) $CeCo_{1-x}Sb_2$ (space group *P*4/*nmm*, $a = 0.3878$ nm and $c = 0.9849$ nm), and $CeCo_{1.33}Sb_2$ (possible space group *Ccc*2, $a = 0.6083$ nm, $b = 0.60118$ nm and $c = 1.04596$ nm). The homogeneity range of CoSb phase is about 2.0 at.% Sb. The solubilities for the other single-phase regions were not observed.

Acknowledgements

The work was supported by the National Natural Science Foundation of China (No. 50471108) and Shenzhen Science and Technology Research Grant (No. 200726).

References

[1] D.T. Morelli, T. Caillat, J.P. Fleurial, A. Borshchevsky, J. Vandersande, B. Chen, C. Uher, Phys. Rev. B 51 (1995) 9622.
[2] T. Caillat, A. Borshchevsky, J.P. Fleurial, J. Appl. Phys. 80 (1996) 4442.
[3] G.S. Nolas, D.T. Morelli, T.M. Tritt, Annu. Rev. Mater. Sci. 29 (1999) 89.
[4] G.S. Nolas, J.L. Cohn, G.A. Slack, Phys. Rev. B 58 (1998) 164.
[5] J.Q. Li, X.W. Feng, J.L. Liang, Y.X. Jian, F.S. Liu, J. Alloys Compd. 439 (2007) 143.
[6] L.M. Zeng, L.T. Yang, X.J. Xu, X.Z. Wei, J. Alloys Compd. 403 (2005) 124.
[7] O. Sologub, P. Salamakha, J. Alloys Compd. 285 (1999) L16.
[8] S.I. Chykhrij, V.B. Smetana, Inorg. Mater. 42 (5) (2006) 503.
[9] TOPAS, General Profile and Structure Analysis Software for Powder Diffraction Data, V2.0, Bruker AXS, Karlsruhe, Germany, 2000.
[10] C.H. Wu, Y.C. Chuang, X.M. Jin, X.H. Guan, Z. Metallkde. 82 (1991) 621.
[11] H. Okamoto, J. Phase Equilib. 12 (1991) 244–245.
[12] A. Borsese, G. Borzone, D. Mazzone, R. Ferro, J. Less-Common Met. 79 (1) (1981) 57.
[13] K.H.J. Buschow, J. Less-Common Met. 37 (1974) 91.
[14] A. Leithe-Jasper, P. Rogl, J. Alloys Compd. 204 (1994) 13.
[15] R.T. Macaluso, D.M. Wells, R.E. Sykora, T.E. Albrecht-Schmitt, et al., J. Solid State Chem. 177 (2004) 293.
[16] A.A. Coelho, J. Appl. Crystallogr. 36 (2002) 86.
[17] X.W. Feng, J.Q. Li, F.S. Liu, R.M. Luo, Intermetallics 16 (2008) 322.
[18] Z.G. Mei, W. Zhang, L.D. Chen, J. Yang, Phys. Rev. B 74 (2006) 153202.
[19] P. Villars, L.D. Calvert, Pearson's Handbook of Crystallographic Data for intermetallic phase, 2nd ed., ASM International, Materials Park, OH, 1997.